



Science Arts & Métiers (SAM)

is an open access repository that collects the work of Arts et Métiers Institute of Technology researchers and makes it freely available over the web where possible.

This is an author-deposited version published in: <https://sam.ensam.eu>
Handle ID: <http://hdl.handle.net/10985/17420>

To cite this version :

Pierre BEAUREPAIRE, Cécile MATTRAND, Nicolas GAYTON, Jean-Yves DANTAN - Tolerance Analysis of a Deformable Component Using the Probabilistic Approach and Kriging-Based Surrogate Models - ASCE-ASME Journal of Risk and Uncertainty in Engineering Systems, Part A: Civil Engineering - Vol. 4, n°3, p.04018028 - 2018

Any correspondence concerning this service should be sent to the repository

Administrator : scienceouverte@ensam.eu



1 **Tolerance analysis of a deformable component using the**
2 **probabilistic approach and Kriging-based surrogate**
3 **models**

4 P. Beaurepaire,¹ C. Mattrand,² N. Gayton,³ J.-Y. Dantan⁴

5 **ABSTRACT**

6 Tolerance analysis is a key issue in proving the compatibility of manufactur-
7 ing uncertainties with the quality level of mechanical systems. For rigid and
8 isostatic systems, multiple methods (worst case, statistical or probabilistic ap-
9 proaches) are applicable and well established. Recent scientific developments
10 have brought enhancements for rigid over-constrained systems, using probabilis-
11 tic and optimization based methods. The consideration of non-rigid systems is
12 more complex, since large-scale numerical model must be taken into account for
13 an accurate prediction of the quality. The aim of the present paper is the illustra-
14 tion of the probabilistic tolerance analysis approach for an industrial application

¹Assistant professor, Université Clermont Auvergne, CNRS, SIGMA-Clermont, Institut Pascal, Campus de Clermont-Ferrand / Les Cézeaux, 27 rue Roche Genès, CS 20265, 63175 Aubière Cedex, France, pierre.beaurepaire@sigma-clermont.fr

²Assistant professor, Université Clermont Auvergne, CNRS, SIGMA-Clermont, Institut Pascal, Campus de Clermont-Ferrand / Les Cézeaux, 27 rue Roche Genès, CS 20265, 63175 Aubière Cedex, France, cecile.mattrand@sigma-clermont.fr

³Professor, Université Clermont Auvergne, CNRS, SIGMA-Clermont, Institut Pascal, Campus de Clermont-Ferrand / Les Cézeaux, 27 rue Roche Genès, CS 20265, 63175 Aubière Cedex, France, nicolas.gayton@sigma-clermont.fr

⁴Professor, LCFC, Arts et Métiers, ParisTech Metz, 4 rue Augustin Fresnel, 57078 Metz Cedex 3, France, jean-yves.dantan@ensam.eu

15 involving deformable parts. The distributions associated with the dimensions of
16 the components are identified using real components collected from the assembly
17 lines. A nonlinear finite element model is used to predict the mechanical behav-
18 ior. A reliability analysis is performed in order to compute the defect probability
19 and estimate the quality of the products. A Kriging-based surrogate model is
20 used to reduce the numerical efforts required for the reliability analysis.

21
22 *Keywords:* Tolerance analysis; Defect probability estimation; System reliabil-
23 ity; Kriging-based surrogate model, Wiping system

24 INTRODUCTION

25 Engineers are aware that uncertainties in the dimensions of manufactured
26 products cannot be avoided, i.e. mechanical components manufactured on the
27 same assembly line using the same tools and the same raw materials have slightly
28 different shapes; and their dimensions are also different from the designer's tar-
29 get. Tolerance analysis offers a rational framework to study such uncertainties,
30 and enables engineers to guarantee that the quality resulting from the produc-
31 tion process remains acceptable. Consequently, production wastage and global
32 manufacturing costs are considerably reduced.

33 It is assumed that the behavior of a mechanical system is fully characterized by
34 a finite set of parameters \mathbf{X} , which are associated with the deviations between the
35 ideal geometry and the geometry of real components; the shape of the components
36 is parameterized; and the vector \mathbf{X} has a finite size. The response of the system
37 Y is described using the functional characteristics (Nigam and Turner 1995); its
38 expression is of the form:

$$39 \quad Y = f(\mathbf{X}) \quad (1)$$

40 where f denotes the response function of the mechanical component.

41 Tolerance analysis can be performed by considering the upper and lower
42 bounds of the functional characteristic expressed in Equation (1). The system is
43 functional as long as its response is between these two bounds. Two strategies
44 are applicable to deal with the geometric deviations (Chase and Parkinson 1991;
45 Greenwood and Chase 1987; Nigam and Turner 1995).

- 46 1. With the **worst case approach**, each dimension X_i is characterized by
47 an upper and a lower bound; and the configuration leading to the worse
48 performance is identified. The tolerance intervals of the dimensions are
49 adjusted in order to guarantee that the component is functional for the
50 worst case (i.e. that the functional characteristics are between the prede-
51 fined bounds for all the possible values of \mathbf{X}).
- 52 2. The **statistical approach** consists of introducing a probabilistic model
53 for the dimensions, and uncertainties are subsequently propagated to the
54 response of the mechanical component. The function characteristic may
55 be outside the predefined bounds; this is tolerated as long as such events
56 remain rare and the frequency of occurrence is controlled. The objective
57 of the tolerance analysis is the determination of this occurrence proba-
58 bility, which is referred to as the defect probability. It provides a metric
59 associated with the quality of the production, which is often expressed in
60 parts per million (ppm) or in parts per billion (ppb) for systems manu-
61 factured by Valeo VWS (the industrial partner in this study). The worst
62 case approach is more conservative, which leads to excessively tight tol-
63 erance intervals and higher manufacturing costs (Hong and Chang 2002;
64 Roy et al. 1991); the statistical approach is therefore used here.

65 During the last two decades, three main issues have been addressed by the
66 tolerance analysis community for the statistical approach. Issue 1 concerns the

67 modeling of random dimensions by probability distributions. Tolerance analysis
68 is commonly performed in the design stage to predict defect probability, and the
69 tolerance intervals are adjusted to meet predefined quality requirements. One of
70 the major challenges is the lack of information at this stage, since parts are not
71 available and it is hence not possible to use measurements of the uncertain dimen-
72 sions to identify their distributions. As a result, assumptions must be introduced
73 into the uncertainty model (using, for instance, feedback obtained with similar
74 components). A possible strategy consists of modeling each dimension with a
75 uniform distribution inside the tolerance interval (Greenwood and Chase 1987).
76 However, this approach may be conservative, and alternative strategies are appli-
77 cable, such as the use of centered or shifted Gaussian distributions (Evans 1975;
78 Scholtz 1995). The uncertainty model may also be defined by means of a dynamic
79 approach (Gayton et al. 2011) when considering batch production. A multi-level
80 model is introduced and the dimensions are modeled using Gaussian distribu-
81 tions. The parts in the same batch have identical mean and standard deviation
82 for all their dimensions. These moments are modeled as random variables, which
83 introduces a second level of uncertainty (Gayton et al. 2011; Scholtz 1995). All
84 these models require assumptions which have considerable consequences on defect
85 probability prediction. The second major issue (issue 2) is the tolerance analysis
86 in case of over-constrained mechanical systems. Equation (1) is not applicable to
87 such problems, as the functional requirement involves the uncertain dimensions
88 of the components, but also gap variables, which may be associated with the dis-
89 tance between the components of the assembly. It is not possible for the designer
90 to set the value of these variables, and they are not characterized by a probabili-
91 ty density function. As the gaps cannot be modeled using random variables nor
92 design variables, they are referred to as *free variables* in this manuscript. The for-
93 mulation of the tolerance analysis problem with gap variables is described e.g. in

94 (Dantan and Qureshi 2009). This is a challenging task, as the identification of an
95 explicit expression of the functional characteristic is in general not possible. For
96 over-constrained systems, multiple contact configurations are possible, leading to
97 multiple candidate values of the functional characteristic. Specific methods have
98 been proposed to identify appropriate contact configurations and compute the
99 defect probability (Dumas et al. 2015; Qureshi et al. 2012). However, tolerance
100 analysis of over-constrained systems remain a challenging task. The last issue
101 (issue 3) concerns the tolerance analysis of systems with deformable parts; the
102 compliance of the components is explicitly considered by introducing a mechani-
103 cal model, obtained for instance using the finite element method (see e.g. (Gordis
104 and Flannelly 1994; Liu and Hu 1996; Söderberg et al. 2006)). Liu and Hu (1997)
105 showed that dimensional variation has little effect on the stiffness of the compo-
106 nents, and a deterministic model can be used for their mechanical behavior. This
107 strategy, known as the influence coefficients method, has been applied with suc-
108 cess to multiple problems, see e.g. (Dahlström and Lindkvist 2006; Li et al. 2004;
109 Lindau et al. 2015). The method is applicable only if (i) the coefficient of varia-
110 tion associated with the uncertain dimensions is sufficiently small (in order they
111 have no effects on the stiffness matrix); (ii) the materials behavior is linear (or
112 the strain is sufficiently small to have a linear material behavior).

113 The Monte Carlo Simulation is widely used to compute the probability of
114 defect, as this method is applicable to non-linear models and non-Gaussian dis-
115 tributions. However, the Monte Carlo method requires considerable numerical
116 efforts when the defect probability is low or when a large scale model is used.
117 Advanced reliability methods, such as the First and Second Order Reliability
118 Method (FORM, SORM) or importance sampling can be used to reduce these
119 numerical efforts (Lemaire 2010).

120 The present paper deals with the implementation of an industrial tolerance

121 analysis application. The problem is the prediction of the defect probability of a
122 deformable wiper blade system subjected to shape and material uncertainty. In
123 this work, the three issues discussed above are considered with great attention.
124 The manufacturing of these components started a few years ago and it is therefore
125 possible to directly measure their dimensions. The problem of the identification
126 of the distribution (issue 1) is hence simplified, as data are available and can
127 be used to identify the most suitable distribution for each dimension. The addi-
128 tional complexity introduced by free variables (issue 2) is addressed by calibrating
129 a response surface, which is subsequently used to eliminate these variables with
130 reduced computational efforts. For the tolerance analysis of such a component,
131 the functional requirements are obtained directly from the structural response.
132 The influence of the uncertain dimensions on the stiffness matrix cannot be ne-
133 glected (and has to be fully considered). The simplifying hypothesis used in the
134 literature for the tolerance analysis of deformable components (issue 3) is not ap-
135 plicable here, and multiple finite element simulations are required to perform the
136 reliability analysis and compute the defect probability. An advanced simulation
137 method is used to perform this analysis with acceptable numerical efforts; it relies
138 on the use of Kriging-based surrogate model (Echard et al. 2011; Echard et al.
139 2013; Fauriat and Gayton 2014).

140 This manuscript is structured as follows: the considered industrial problem in
141 described in Section 2; the stochastic structural model is described in Section 3
142 with a presentation of the modeling of uncertainties from profile measurements.
143 The proposed surrogate model-based methodology is next discussed in the fourth
144 section before presenting the results in Section 5. The article closes with conclu-
145 sions and perspectives in Section 6.

146 **DESCRIPTION OF THE INDUSTRIAL PROBLEM**

147 This study concerns the tolerance analysis of a wiper system. Such compo-
148 nents are used in the automotive industry to remove water and debris from the
149 windshield. The methods developed here are applied to flat blade technology.
150 The blade is fixed at its center to the wiper arm, which applies an alternating
151 rotation movement (see Figure 1) and maintains the contact between the blade
152 and the windshield.

153 The blade is mainly composed of metallic splines and of a rubber profile that
154 is the focus of this paper. The shape of the splines matches the curvature of the
155 windshield; they provide sufficient stiffness to the assembly, preventing an uneven
156 distribution of the pressure at the contact between the blade and the windshield.
157 The rubber profile includes multiple sub-components (see Figure 2):

- 158 • the lips ensure wiping and windshield cleaning;
- 159 • the hinge, which controls the deformation of the blade and the contributes
160 to reverse the blade (when the wiper reaches the end of its travel and turns
161 back);
- 162 • the heel, which locks the fir to the blade assembly.

163 During wiping, the profile is considerably strained; the fir and the heel come
164 into contact as shown in Figure 2. The mechanical deformation of the rubber
165 profile during the wiping cycle depends on the tip force, the friction coefficient
166 between the windshield and the rubber, the material properties and the geomet-
167 rical characteristics. A good control of blade profile deformation prevents:

- 168 • fast deterioration of the rubber leading to ridge defect on the windshield
169 as shown in Figure 3a;
- 170 • return defects generated by particular geometrical conditions of the rubber
171 profile as shown in Figure 3b.

172 The performance of the system is evaluated from the structural response,
173 i.e. fluid-structure interactions are not considered here, and therefore the multi-
174 physics problem is transformed into a mechanical problem. The two first per-
175 formance criteria of the wiper system are determined using the contact angle α
176 (*i.e.* the angle between the lips of the fir and the windshield) and the locking
177 angle β (measured at the contact point between the fir and the heel, as shown
178 in Figure 2). The maximum strain ϵ_{max} of the rubber hinge is used as a third
179 performance criterion, since it may be an indicator of the aging of the rubber.

180 This paper is focused on the investigation of the consequences of geometri-
181 cal and material uncertainties on the performance of a wiper system. Only the
182 uncertainties associated with the rubber profile are considered. Consequently,
183 the aim of this paper is the evaluation of the system probability that α , β and
184 ϵ_{max} fall outside functional ranges, each quantity depending on random geometry,
185 characterized by parameters grouped in vector \mathbf{D} , and the material properties,
186 characterized by parameters grouped in vector \mathbf{P} .

187 This work also enables us to obtain feedback on the actual distribution of the
188 dimensions of the wiper blade. This is an important matter, since in practice
189 designers lack this information to estimate the quality level associated with a
190 component. The study provides an opportunity to analyze real part data, iden-
191 tify the distribution associated with the various dimensions, determine whether
192 the assumptions usually made during design are realistic, etc. The dependence
193 between the dimensions is an interesting element, too. Indeed, the profiles are
194 manufactured using an extrusion process, which introduces correlation between
195 the dimensions. The information collected here may be re-used in the future in
196 the definition of the random variable set for wiper profiles manufactured using
197 the same process.

198 **STOCHASTIC STRUCTURAL MODEL**

199 **Probabilistic model**

200 *Characterization of uncertain parameters*

201 The components are manufactured using a rubber extrusion process, and the
202 profiles are subsequently cut to obtain blades of the required length. The uncer-
203 tainties associated with the length of the blade are not considered here, and thus
204 the geometry of the component is defined by the cross-section of the blade. The
205 reference cross-section, as it appears for instance in the computer-aided design
206 model, is shown in Figure 4a. The manufacturing process introduces unavoidable
207 geometrical deviations, and the actual geometry of a wiper blade differs from the
208 reference geometry. A manufactured part is shown in Figure 4b and geometrical
209 deviations are perceptible. The shape of the rubber profile is frequently controlled
210 in the factories to quantify these geometric deviations; a video measurement tool
211 is used to avoid the part deformation during its size control. The shape of the
212 observed cross-section is complex, and the preparation of a geometrical model
213 capturing fully the deviation with respect to the drawings would be a challenging
214 task. A simplified non-ideal cross-section is introduced; it is fully described using
215 a finite number of parameters \mathbf{D} as shown in Figure 5. In total, 44 different
216 quantities are determined to characterize the reference cross-section of the blade
217 (length and width at various locations, fillet radii, *etc*). A probabilistic approach
218 is used and a random variable is introduced for each geometrical parameter.

219 It is assumed that the uncertainties can be fully characterized using the linear
220 correlation matrix and marginal distributions. Alternative strategies may be
221 considered to account for the correlation between the dimension, such as for
222 instance copulas (see e.g. (Mai and Scherer 2012; Schölzel and Friederichs 2008)).
223 However, such approaches are not used here.

224 Initially, a set of candidate distributions is arbitrarily selected. Only four
 225 candidate distributions are use here but additional distributions may be included
 226 without modifying the proposed procedure. In the study, the dimensions may
 227 follow either a uniform, exponential, normal or lognormal distribution. In each
 228 case, it is necessary to identify the parameters of the distribution leading to
 229 the best match with the data obtained from the factory. These parameters are
 230 obtained by maximizing the likelihood function, which is expressed as:

$$231 \quad L(D_i^{(1)}, D_i^{(2)}, \dots, D_i^{(45)}, \mathbf{p}, \mathcal{D}) = \prod_{j=1}^{45} f_{D_i}(D_i^{(j)}, \mathbf{p}, \mathcal{D}) \quad (2)$$

232 where $D_i^{(j)}$, $j = 1 \dots 45$ denotes the measurements available for the i^{th} dimension of
 233 the wiper blade, which are used to identify the distribution of the corresponding
 234 random variable; in total, 45 dimension measurements are used to identify the
 235 distributions. \mathbf{p} is a vector grouping all the distribution parameters (*e.g.* mean,
 236 standard deviation, bounds), f_{D_i} denotes the probability density function of the
 237 random variable D_i and \mathcal{D} represents the considered distribution (i.e. either the
 238 normal, uniform, exponential or lognormal distribution). The value of the terms
 239 of \mathbf{p} is selected such that L is maximized.

240 The most suitable distribution is then selected using the Akaike Information
 241 Criterion (AIC) (Akaike 1974):

$$242 \quad AIC(D_i^{(1)}, \dots, D_i^{(45)}, \hat{\mathbf{p}}, \mathcal{D}) = -2 \ln L(D_i^{(1)}, \dots, D_i^{(45)}, \hat{\mathbf{p}}, \mathcal{D}) + 2q(\mathcal{D}) \quad (3)$$

243 where $\hat{\mathbf{p}}$ denotes the optimal value of the distribution parameters (which maximize
 244 Equation (2)), and q is the number of parameters associated with the distribution.
 245 For an exponential distribution, q is equal to one (and in this case $\hat{\mathbf{p}}$ is a scalar);
 246 otherwise q is equal to two (and $\hat{\mathbf{p}}$ is a vector with two terms). The distribution

247 \mathcal{D} associated with the maximum value of the AIC leads to the best fit with the
248 available data, and is subsequently used in the probabilistic model.

249 This operation is repeated for all the dimensions considered and, in total, 44
250 distributions are identified using the procedure described above. It is observed
251 that either the normal distribution or uniform distribution maximize the AIC for
252 most of the dimensions; the lognormal distribution is occasionally used, but it
253 remains rare; the exponential distribution is never used.

254

255 The manufacturing process has a strong influence on the dependence between
256 the uncertain parameters, as physical phenomena are involved and impact all
257 the dimensions. For instance, the rubber may expand after extrusion, causing
258 a positive correlation between the dimensions H_2 and H_4 indicated in Figure 5,
259 whereas it causes a negative correlation between the dimensions H_1 and H_2 . Fig-
260 ure 6 represents a scatterplot of these dimensions, the correlation between the
261 dimensions is clearly visible. In this work, samples of the uncertain parameters
262 are available and for each measurement, all the dimensions are determined on
263 the same part. Thus, the correlation matrix can be directly computed from the
264 measurements.

265

266 The vector \mathbf{P} gathers the uncertainties associated with the material param-
267 eters. These coefficients are used to define a probabilistic hyperelastic model of
268 the mechanical behavior of rubber. In total, two independent random variables
269 are used to characterize the material uncertainties. The details of this model are
270 not discussed here for confidentiality reasons.

271 *Isoprobabilistic transformation*

272 Most reliability algorithms are applied in the so-called *standard normal space*,
 273 where all the random variables are independent and have a standard normal dis-
 274 tribution, with a zero mean and a unitary standard deviation. An isoprobabilistic
 275 transformation is applied to each random variable; it is expressed as:

$$276 \quad z_i = \Phi^{-1} (F_{D_i} (D_i)) \text{ for } i = 1, \dots, 44 \quad (4)$$

277 where Φ^{-1} denotes the inverse of the standard normal cumulative density function,
 278 F_{D_i} is the cumulative distribution function associated with the variable D_i and
 279 z_i denotes the random variables expressed using its original distribution and its
 280 counterpart in the standard normal space, respectively.

281 In case the variables D_i and D_j are correlated before the transformation de-
 282 scribed in Equation (4), the variables z_i and z_j are correlated as well, and ρ'_{ij}
 283 denotes their correlation coefficient. The approximation of ρ'_{ij} available in (Liu
 284 and Der Kiureghian 1986) are used here.

285 In the standard normal space the covariance matrix and the correlation matrix
 286 are identical and defined as:

$$287 \quad \Sigma' = [\rho'_{ij}]_{1 \leq i \leq 44, 1 \leq j \leq 44} \quad (5)$$

288 The Karhunen-Loève (Karhunen 1947; Loève 1977) transform is used to decor-
 289 relate the random variable, it is expressed as:

$$290 \quad \mathbf{z} = \sum_{i=1}^{44} \xi_i \sqrt{\lambda_i} \phi_i \quad (6)$$

291 where $\mathbf{z} = [z_1, \dots, z_{44}]$; ξ_i , $i = 1 \dots 44$ denotes independent variables with a standard
 292 normal distribution, and λ_i and ϕ_i denote respectively the eigenvalues and the

293 eigenvectors associated with the matrix Σ' .

294 In Equation (6), the eigenvalues are sorted in descending order, and hence the
295 first few terms have a major contribution to the variance of the set \mathbf{z} . Figure 7
296 shows the percentage of explained variance, expressed in terms of the total num-
297 ber of considered eigenvalues. The Karhunen-Loève expansion can be truncated
298 to reduce the total number of random variables involved in the problem, with
299 reduced loss of accuracy regarding the covariance matrix of the random variable
300 set. In this work, the Karhunen-Loève expansion is performed using the 10 first
301 terms of Equation (6). We have $\sum_{i=1}^{10} \lambda_i / \sum_{i=1}^{44} \lambda_i > 0.95$ and hence at least 95%
302 of the variance of \mathbf{z} is accounted for. The Karhunen-Loève expansion allows us
303 to considerably reduce the dimensionality of the problem because the random
304 variables are strongly correlated.

305 **Mechanical model**

306 A finite element model is prepared to predict the behavior of the blade and
307 determine the contact angle α , the locking angle β and the maximum strain ε_{max} .
308 The boundary conditions applied to the structure need to be identified to set up
309 the mechanical model. The reaction forces at the contact and the coefficient of
310 friction between the blade and the windshield are the key inputs.

311 The contact forces are not constant along the wiper blade; they are therefore
312 expressed in terms of the x-coordinate. This variation of the contact forces is
313 caused by the geometry of the wiping blade and the curvature of the windshield.
314 It is observed that the maximum force is obtained in the middle of the blade, as
315 the connection with the wiper arm is situated in this location. Figure 8a shows
316 the distribution of the forces with respect to the x-coordinate. These curves are
317 obtained via a beam model; the details of its implementation are not discussed
318 herein. The inclination of the wiper on the windshield causes aerodynamic effects

319 on its movement. During the upward movement, the wiping benefits from positive
320 airflow effects, and hence the applied load is lower. However, the downward
321 movement is adversely affected by the airflow, which causes a higher load. As a
322 result, two distinct types of forces are presented. The first curve (dashed black
323 line) corresponds to the efforts during wiping in the upwards direction and the
324 second curve (continuous grey line) to those in the downward direction. The
325 maximum load F_{max} is reached at the center of the blade for the wiping in the
326 upwards direction; the minimum load F_{min} is reached at two different positions
327 for the wiping in the upwards direction.

328 The friction coefficient between the blade and the windshield varies along
329 the wiper length as well, and is influenced by the velocity of the blade. The
330 friction coefficient increases as the velocity decreases. During wiping, the outer
331 portion covers a greater distance and therefore has a higher speed than the inner
332 part. In the mechanical model, the friction coefficient μ follows a linear curve
333 along the length of the wiper, as shown in Figure 8b. Indeed, the difference in
334 values is explained by the fact that the speed is not the same along the whole
335 length of the wiper. In practice, stick-slips may be observed, leading to a more
336 complex behavior. The linear evolution of the coefficient of friction is a first-
337 order approximation and more complex models are not used here for the sake
338 of simplicity. A change in the friction model would not affect the tolerancing
339 methodology. The minimum and maximum values of the coefficient of friction
340 μ_{min} and μ_{max} are reached at the ends of the blade.

341 The finite element method is accurate only if the elements have roughly the
342 same size in all directions (i.e. the same length, width and height). The total
343 length of the wiper blade is approximately 100 times greater than its width or
344 eight. A three dimensional mesh would hence include a large number of elements.
345 The model is non-linear since the rubber has hyperelastic properties, large dis-

346 placements are observed and the contact with the windshield is accounted for.
347 Hence, the problem is not suitable for the application of a three-dimensional
348 model, as it would involve multiple inversions of a large scale stiffness matrix.
349 A simplified two-dimensional mechanical model is used instead, as shown in Fig-
350 ure 9. Each simulation is associated with a specific position on the blade, i.e. with
351 a specific x-coordinate, since the boundary conditions are expressed in terms of
352 the x-coordinate. Thus, the corresponding load and coefficient of friction need
353 to be injected into the model; they are selected as shown in the curves repre-
354 sented in Figure 8. Multiple simulations are performed in order to account for
355 the variation in the response of the blade with respect to the x-coordinate, and
356 wiping in the upwards and the downwards directions also needs to be accounted
357 for. Each finite element simulation takes one to ten minutes, depending on the
358 non-linearity (contact configuration, material parameters, etc.).

359 **Performance functions**

360 Performance functions are introduced for the reliability analysis; their for-
361 mulation involves the functional requirements. The value of the performance
362 function is less than zero in the failure domain, i.e. in the case where one of
363 the functional requirements is not fulfilled, and this function is greater than zero
364 otherwise. As discussed in Section 3, the boundary conditions are expressed with
365 respect to the x-coordinate in the blade. As a result, the performance functions
366 are also expressed in terms of the x-coordinate. The wiper blade is assumed to
367 be functional at a given position with x as a coordinate if the maximum strain
368 is below a predefined value; the contact angle and the locking angle are within a
369 predefined range. Hence, five normalized performance functions are introduced,
370 they are defined as:

$$\begin{aligned}
g_1(\mathbf{D}, \mathbf{P}, x) &= \frac{\varepsilon_{max}^u - \varepsilon_{max}(\mathbf{D}, \mathbf{P}, x)}{\varepsilon_{max}^u} \\
g_2(\mathbf{D}, \mathbf{P}, x) &= \frac{\alpha(\mathbf{D}, \mathbf{P}, x) - \alpha^l}{\alpha^l} \\
g_3(\mathbf{D}, \mathbf{P}, x) &= \frac{\alpha^u - \alpha(\mathbf{D}, \mathbf{P}, x)}{\alpha^u} \\
g_4(\mathbf{D}, \mathbf{P}, x) &= \frac{\beta(\mathbf{D}, \mathbf{P}, x) - \beta^l}{\beta^l} \\
g_5(\mathbf{D}, \mathbf{P}, x) &= \frac{\beta^u - \beta(\mathbf{D}, \mathbf{P}, x)}{\beta^u}
\end{aligned} \tag{7}$$

where ε_{max} , α and β denote the functional requirements, *i.e.* the maximum strain, the contact angle and the locking angle, respectively; these functions are evaluated in terms of the position along the rubber profile x and in terms of a particular value of the uncertain dimensions \mathbf{D} and material parameters \mathbf{P} . ε_{max}^u is the maximum admissible strain; α^u and β^u are the maximum admissible contact and locking angles, respectively; α^l and β^l are the minimum admissible contact and locking angles, respectively.

The functions described in Equation (7) can be used to describe the behavior of the wiper blade locally, at the point with the coordinate x , whereas the functionality of the wiper must be determined globally at the level of the system. For a set of random variables \mathbf{D}, \mathbf{P} (geometric and material, respectively), the profile is functional if it leaves no visible wiping defects on the windshield, *i.e.* all the performance functions must be greater than zero for all the possible values of x .

To solve the reliability problem, the performance functions can be formulated without dependence on the x -coordinate. They are expressed as:

$$G_i(\mathbf{D}, \mathbf{P}) = \min_{x_{min} < x < x_{max}} g_i(\mathbf{D}, \mathbf{P}, x) \text{ for } i = 1 \dots 5 \tag{8}$$

389 where G_i denotes the newly introduced performance function, and x_{min} and x_{max}
390 denote the lower and upper bounds of the x-coordinate, respectively. System
391 reliability is used here and five performance functions are defined in Equation (7).
392 Therefore, the procedure described in Equation (8) is applied five times.

393 **SOLUTION STRATEGY**

394 Defect probability is expressed as a probability of failure, and a reliability
395 algorithm is thus used. The proposed procedure needs to deal efficiently with the
396 two following points.

- 397 • An optimization problem must be solved each time a performance func-
398 tion is evaluated, as indicated in Equation (8). A design of experiments is
399 performed with respect to the parameters of the boundary conditions, i.e.
400 the contact force and the coefficient of friction. Response surfaces are cali-
401 brated and subsequently used to identify the minimum of the performance
402 function with a reduced number of calls to the finite element model. The
403 procedure is described in Section 4.
- 404 • The total number of calls to the performance functions should be reduced
405 since a non-linear FE model is involved. An advanced procedure, based
406 on AK methods, is implemented to determine the defect probability with
407 reduced numerical efforts; this algorithm is described in details in Section 4

408 **Evaluation of the performance functions**

409 The identification of the minimum of the performance function expressed by
410 Equation (8) is numerically demanding. A non-linear finite element simulation is
411 required, and the identification of the minimum is thus numerically prohibitive.

412 Surrogate models are used to reduce the computational efforts associated with
413 Equation (8). A response surface is calibrated for each performance function and

414 for each realization of the random variables (generated by the reliability algo-
 415 rithm). The response surfaces involve as input parameters the coefficient of fric-
 416 tion and the force applied as a boundary conditions. The calibration set consists
 417 of nine samples selected such that they cover the range of variation of these pa-
 418 rameters. In the case where the force F is near its lower bound, the coefficient
 419 may vary over a large range of values, and hence the design of experiments points
 420 are scattered. In the case where the applied force is near its upper bound, the
 421 coefficient of friction varies over a narrower range, and the design of experiments
 422 points are concentrated. Finite element simulations are performed using realiza-
 423 tions of the random variables generated by the reliability algorithm, which define
 424 the geometry of the model. For each realization, nine simulations are performed;
 425 the boundary conditions are set for the nine pairs $(\mu^{(k)} - F^{(k)})$, $k = 1 \dots 9$, as
 426 shown in Figure 10. The position in the wiper is not considered at this stage
 427 and only the parameters associated with the boundary conditions (i.e. μ and
 428 F) are involved in this design of experiments. In case the reliability procedure is
 429 performed using N samples; $9N$ finite element simulations are performed in total.

430

431 For each realization of the random variables, the performance functions g_i , $i =$
 432 $1 \dots 5$ are subsequently approximated by second order polynomials:

$$433 \quad g_i(\mathbf{D}^{(j)}, \mathbf{P}^{(j)}, x) \simeq Q_i^{(j)}(F(x), \mu(x)) \quad (9)$$

434 where $Q_i^{(j)}$ denotes second order polynomials. Unlike surrogate model based
 435 reliability algorithms (see e.g. (Bucher and Bourgund 1990)), the polynomials
 436 $Q_i^{(j)}$ are not expressed with respect to the random variables and the polynomial
 437 coefficient need to be determined for each realization. The experience showed
 438 that the responses of the finite element model are quasi-linear with respect to the

439 force and the coefficient of friction (for the considered range of variation of these
440 parameters). Therefore, second order polynomials provide a suitable framework
441 to approximate the mechanical response, as they account for the linear trend and
442 the slight non-linearities. These polynomials are solely used to reduce the efforts
443 associated with the optimization problem described in Equation (8).

444 The quality of the polynomial fit is checked using cross-validation. The ap-
445 plied strategy consists of excluding a sample-result pair from the calibration set,
446 then calibrating the response surface using the remaining data and using it to
447 predict the outcome of the finite element model associated with the excluded
448 sample. As the response is known, the error associated with the surrogate model
449 can be estimated. The method is repeated multiple times, for all the nine de-
450 sign of experiments samples and for multiple realizations of the random variables.
451 The coefficient of determination for prediction R^2 is determined; it provides an
452 appropriate metric of the quality of the fit (Myers et al. 2008). All the design
453 of experiments points shown in Figure 10 are tested for 100 independent realiza-
454 tions of the random variables, and we obtain $R^2 > 0.99$ for all the performance
455 functions. It can be concluded from the high R^2 values that second-order poly-
456 nomials accurately approximate the response of the finite element models, and in
457 the following all nine design of experiments samples are used for the calibration
458 of the response surface.

459

460 **Reliability analysis using AK methods**

461 Probability evaluation using sampling techniques consists in classifying a large
462 population (obtained using Monte Carlo sampling or any equivalent procedure)
463 into safe and unsafe realizations according to the sign of the performance function
464 $g(\mathbf{x})$, where \mathbf{x} denotes the random variables, i.e. $\mathbf{x}^T = [\mathbf{D}^T, \mathbf{P}^T]$. A schematic

465 representation of the classification between the failure domain and the safe do-
466 main is shown in Figure 11a. Such approaches can become prohibitively expensive
467 in terms of computational effort, especially for low probability evaluations and/or
468 complex numerical performance functions. A possible solution consists of replac-
469 ing the latter with a surrogate model that can be evaluated inexpensively. Active
470 learning and Kriging based methods (AK) use Kriging in an iterative procedure
471 to build a separator of safe and unsafe realizations with only a few well-chosen
472 performance function evaluations. The AK-SYS method (Fauriat and Gayton
473 2014) is used in this application, since a system reliability problem is involved.
474 This algorithm is an adaptation of the AK classification principle for system re-
475 liability evaluation based on Monte Carlo simulation. The classification of the
476 AK-method is decomposed into 5 steps (Echard et al. 2011):

- 477 1. Generation of a Monte Carlo population S of size n_{MC} : $\mathbf{x}^{(1)} \dots \mathbf{x}^{(n_{MC})}$.
478 At this stage none of them are evaluated on the mechanical performance
479 function.
- 480 2. Definition of the initial design of experiments by randomly select N points
481 in S . Compute all of the N points on the mechanical model.
- 482 3. Computation of the Kriging surrogate model according to the design of
483 experiments;
- 484 4. Prediction by Kriging on S and estimation of the probability of failure;
- 485 5. Identification of the best next point in S to evaluate on the performance
486 function if the stopping criterion is not yet reached.

487 A schematic representation of the AK method is shown in Figure 11b.

488 The main originality of the AK method is the preliminary choice of the pop-
489 ulation S . In the case of a unique performance function, the learning criterion is

490 defined by:

$$491 \quad U(\mathbf{x}^{(j)}) = \frac{|\hat{g}(\mathbf{x}^{(j)})|}{\sigma_g(\mathbf{x}^{(j)})} \text{ for } j = 1 : n_{MC} \quad (10)$$

492 where $\hat{g}(\mathbf{x}^{(j)})$ and $\sigma_g(\mathbf{x}^{(j)})$ are respectively the Kriging prediction and standard
 493 deviation estimation. Under Gaussian assumptions, $U(\mathbf{x}^{(j)})$ is linked to the prob-
 494 ability that $\hat{g}(\mathbf{x}^{(j)})$ would not have the same sign as $g(\mathbf{x}^{(j)})$. The stopping criterion
 495 is reached when all the points of S are considered to be well classified, *i.e.* when
 496 $\min(\mathbf{x}^{(j)}) > 2$. For system reliability, the AK-SYS method (Fauriat and Gayton
 497 2014) deals with m different performance functions $g_j(\mathbf{x})$ and union probability
 498 is required:

$$499 \quad P_f = \text{Prob}(g_1(\mathbf{x}) \leq 0 \bigcup \dots \bigcup g_m(\mathbf{x}) \leq 0) \quad (11)$$

500 The AK-SYS method is based on the AK-classification principle and the follow
 501 enrichment criterion is adopted as discussed in (Fauriat and Gayton 2014):

$$502 \quad U(\mathbf{x}^{(j)}) = \frac{|\hat{g}_s(\mathbf{x}^{(j)})|}{\sigma_{g_s}(\mathbf{x}^{(j)})} \text{ for } j = 1 : n_{MC} \quad (12)$$

503 where s is the performance function index that minimizes $g_j(\mathbf{x})$. The advantage
 504 procured by this approach is that no calls (or only a small number) will be made
 505 to the true performance functions that have little or no influence on the system
 506 failure domain.

507 In the implementation of the procedure, a constant trend is used for the
 508 Kriging surrogate model, together with a Gaussian isotropic covariance function.
 509 Therefore, three hyperparameters are used in total: the mean value, the variance
 510 and the correlation length. They are identified using the method of the maximum
 511 of likelihood.

512 Figure 12 represents the workflow implemented for the reliability analysis; it
 513 can be described as a double loop approach. The outermost loop is the AK-

514 based reliability method, which iteratively generates realizations of the random
515 variables. The innermost loop evaluates the performance functions associated
516 with the samples generated by the AK method. These functions also involve the
517 x-coordinate. For each realization, a response surface is calibrated and used to
518 eliminate this additional variable.

519 RESULTS

520 Figure 13 shows the variation in defect probability as the AK method is used.
521 In total, approx. 1300 finite element simulations are required to run the proce-
522 dure, as multiple analyses are performed for each evaluation of the performance
523 functions, as discussed in Section 4.

524 During the first few iterations of the procedure, the design of experiments
525 does not include enough samples and the Kriging surrogate models have low
526 fidelity. As a result, the confidence interval associated with the defect probability
527 is wide. During the subsequent iterations, the design of experiments is enriched
528 with additional samples, which improves the fidelity of the surrogate models and
529 reduces the width of the confidence intervals.

530 Defect probability remains below the predefined quality threshold, indicated
531 by a dashed line in Figure 13. The procedure is stopped prematurely, even though
532 it has not fully converged. Indeed, multiple nonlinear analyses are required,
533 which causes excessive numerical efforts. The defect probability is smaller than
534 its threshold value and the confidence interval does not include this threshold
535 value either. It can hence be concluded that the quality requirements are met
536 and no additional simulation is performed. The failure probability is determined
537 by counting the total number of samples in the failure domain using the surrogate
538 model (i.e. the samples with $\hat{g}(\mathbf{x}) \leq 0$). It is assumed that the sample $\mathbf{x}^{(j)}$ is
539 very likely to be well classified in case $U(\mathbf{x}^{(j)}) \geq 2$, the relevance of this threshold

540 value is discussed e.g. in (Echard et al. 2011). This criterion is used to determine
541 the confidence bounds of the failure probability. The lower bound of the failure
542 probability is obtained using the samples in the failure domain with a low chance
543 of misclassification, i.e. the samples with $\hat{g}(\mathbf{x}) \leq 0$ and $U(\mathbf{x}) \geq 2$; the upper
544 bound of the failure probability is determined using the samples in the safe domain
545 with a low chance of misclassification, i.e. the samples with $\hat{g}(\mathbf{x}) > 0$ and $U(\mathbf{x}) \geq$
546 2.

547 The method also enables us to identify the dominant failure mode. This
548 information may be used as an input for quality improvement.

549 CONCLUSIONS

550 A procedure for the tolerance analysis of a deformable system is proposed
551 in this study. The method is used to determine the defect probability associ-
552 ated with an industrial problem: a wiper blade manufactured by Valeo Wiper
553 Systems. The distributions of the uncertain dimensions are estimated directly
554 from measurements obtained from the factory. The performance of the system
555 is obtained from the structural response. A finite element model of the rub-
556 ber blade is prepared; it includes uncertainties in the geometry of the profile.
557 Structural reliability methods are subsequently used to compute the defect prob-
558 ability. The problem is formulated using a *double loop* approach: the outermost
559 loop consists of the reliability analysis and realizations of the random variables
560 are generated. The innermost loop consists of solving an optimization problem
561 for each realization of the random variables. The numerical efforts are reduced
562 using a surrogate model based procedure. In the innermost loop, design of ex-
563 periments is used for each sample and the structural responses are approximated
564 by second order polynomials. The so-called AK methods are used to reduce the
565 numerical efforts associated with the reliability analysis; such algorithm rely on

566 the use of Kriging surrogate models. It is concluded from this study that quality
567 requirements are met by the wiper blade.

568 Two major original features are introduced in this study. Firstly, the distri-
569 butions associated with the dimensions are directly identified from their realiza-
570 tions, obtained from parts collected on the production lines. This strategy also
571 provides the correlation between the dimensions, which is important information
572 that designers often lack. It is necessary to adopt such an approach, based on in-
573 dustrial data, to obtain a realistic estimation of the defect probability. Secondly,
574 the approach is directly deployed on a full scale industrial model. Because of
575 the considerable uncertainties in the dimensions, the stiffness matrix cannot be
576 assumed to be constant, and the influence method is not applicable. A structural
577 reliability algorithm is used instead, and defect probability is computed using AK
578 methods.

579 Future work is geared towards improvements of the geometrical modeling of
580 the wiper blade by considering form defects.

581 **ACKNOWLEDGEMENTS**

582 This research is partially supported by the French Science Agency (ANR)
583 under contract No. ANR-11-MONU-013, which is gratefully acknowledged by
584 the authors.

585 The authors are grateful to Laurent André-Masse and Sébastien Jallet, Valeo
586 VWS, for their collaboration on this study and their assistance with the finite
587 element model. David Turner is gratefully acknowledged for the proofreading of
588 the manuscript.

589 **REFERENCES**

590 Akaike, H. (1974). “A new look at the statistical model identification.” IEEE
591 Transactions on Automatic Control, 19(6), 716–723.

592 Bucher, C. and Bourgund, U. (1990). “A fast and efficient response surface ap-
593 proach for structural reliability problems.” Journal of Structural Safety, 7(1),
594 57–66.

595 Chase, K. W. and Parkinson, A. R. (1991). “A survey of research in the applica-
596 tion of tolerance analysis to the design of mechanical assemblies.” Research in
597 Engineering Design, 3(1), 23–37.

598 Dahlström, S. and Lindkvist, L. (2006). “Variation simulation of sheet metal
599 assemblies using the method of influence coefficients with contact modeling.”
600 Journal of Manufacturing Science and Engineering, 129(3), 615–622.

601 Dantan, J.-Y. and Qureshi, A.-J. (2009). “Worst-case and statistical tolerance
602 analysis based on quantified constraint satisfaction problems and Monte Carlo
603 simulation.” Computer-Aided Design, 41(1), 1 – 12.

604 Dumas, A., Gayton, N., Dantan, J.-Y., and Sudret, B. (2015). “A new sys-
605 tem formulation for the tolerance analysis of overconstrained mechanisms.”
606 Probabilistic Engineering Mechanics, 40, 66 – 74.

607 Echard, B., Gayton, N., and Lemaire, M. (2011). “AK-MCS: an active learning
608 reliability method combining kriging and monte carlo simulation.” Structural
609 Safety, 33, 145–154.

610 Echard, B., Gayton, N., Lemaire, M., and Relun, N. (2013). “A combined im-
611 portance sampling and kriging reliability method for small failure probabilities
612 with time-demanding numerical models.” Reliability Engineering & System
613 Safety, 111, 232 – 240.

614 Evans, D. (1975). “Statistical tolerancing: The state of the art. part ii, methods
615 for estimating moments.” Journal of Quality Technology, 17(1), 1–12.

616 Fauriat, W. and Gayton, N. (2014). “AK-SYS: An adaptation of the AK-MCS
617 method for system reliability.” Reliability Engineering & System Safety, 123(0),
618 137 – 144.

619 Gayton, N., Beaucaire, P., Bourinet, J.-M., Duc, E., Lemaire, M., and Gauvrit, L.
620 (2011). “APTA: Advanced probability - based tolerance analysis of products.”
621 Mécanique et Industrie, 12, 71–85.

622 Gordis, J. and Flannelly, W. (1994). “Analysis of stress due to fastener tolerance
623 in assembled components.” AIAA Journal, 32, 2440–2446.

624 Greenwood, W. and Chase, K. (1987). “A new tolerance analysis method for
625 designers and manufacturers.” Transaction of the ASME, 109–116.

626 Hong, Y. and Chang, T. (2002). “A comprehensive review of tolerancing re-
627 search.” International Journal of Production Research, 40(11), 2425–2459.

628 Karhunen, K. (1947). “Über lineare Methoden in der Wahrscheinlichkeitsrech-
629 nung.” Amer. Acad. Sci., Fennicade, Ser. A, 37, 3–79.

630 Lemaire, M. (2010). Structural Reliability. ISTE, Wiley.

631 Li, Z., Yue, J., Kokkolaras, M., Camelio, J. A., Papalambros, P., and Hu,
632 J. S. (2004). “Product tolerance allocation in compliant multistation assembly
633 through variation propagation and analytical target cascading.” 2004 ASME
634 International Mechanical Engineering Congress and Exposition, Anaheim, CA
635 (November 1320).

636 Lindau, B., Lorin, S., Lindkvist, L., and Söderberg, R. (2015). “Efficient con-
637 tact modeling in nonrigid variation simulation.” Journal of Computing and
638 Information Science in Engineering, 16(1), 011002.

639 Liu, P.-L. and Der Kiureghian, A. (1986). “Multivariate distribution models with
640 prescribed marginals and covariances.” Probabilistic Engineering Mechanics,
641 1(2), 105–112.

642 Liu, S. and Hu, S. (1996). “Variation simulation for deformable sheet metal as-
643 semblies using finite element methods.” Journal of Manufacturing Science and
644 Engineering, 119(3), 368–374.

645 Liu, S. C. and Hu, S. J. (1997). “Variation simulation for deformable sheet metal

646 assemblies using finite element methods.” ASME Journal of Manufacturing
647 Science and Engineering, 119(3), 368374.

648 Loève, M. (1977). Probability Theory. Springer-Verlag, New York, 4th edition
649 edition.

650 Mai, J.-F. and Scherer, M. (2012). Simulating Copulas (Stochastic Models,
651 Sampling Algorithms and Applications), Vol. 4 of Series in Quantitative
652 Finance. World Scientific.

653 Myers, R. H., Montgomery, D. C., and Andersson-Cook, C. M. (2008). Response
654 surface methodology: process and product optimization using designed
655 experiments. Wiley, Jersey, USA.

656 Nigam, S. and Turner, J. (1995). “Review of statistical approaches to tolerance
657 analysis.” Computer-Aided Design, 27(1), 6 – 15.

658 Qureshi, A.-J., Dantan, J.-Y., Sabri, V., Beaucaire, P., and Gayton, N. (2012). “A
659 statistical tolerance analysis approach for over-constrained mechanism based
660 on optimization and monte carlo simulation.” Computer Aided Design, 44(2),
661 132–142.

662 Roy, U., Liu, C., and Woo, T. (1991). “Review of dimensioning and tolerancing:
663 representation and processing.” Computer-Aided Design, 23(7), 466 – 483.

664 Scholtz, F. (1995). “Tolerance stack analysis methods.” Report no., Boeing Tech-
665 nical Report.

666 Schölzel, C. and Friederichs, P. (2008). “Multivariate non-normally distributed
667 random variables in climate research – introduction to the copula ap-
668 proach.” Nonlinear Processes in Geophysics, 15(5), 761–772.

669 Söderberg, R., Lindkvist, L., and Dahlström, S. (2006). “Computer-aided robust-
670 ness analysis for compliant assemblies.” Journal of Engineering Design, 17(5),
671 411–428.

LIST OF FIGURES

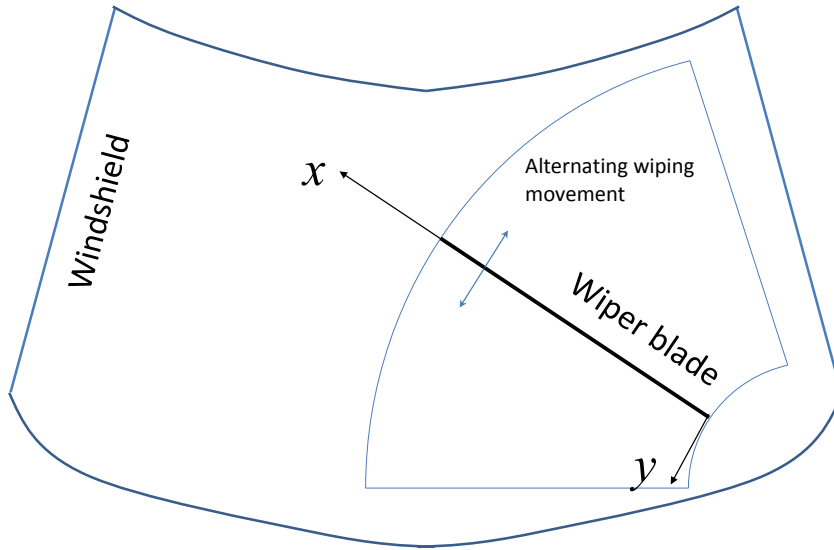


FIG. 1: Alternating movement of the wiper system. The local coordinate system, associated with the wiper blade, is indicated by the arrows.

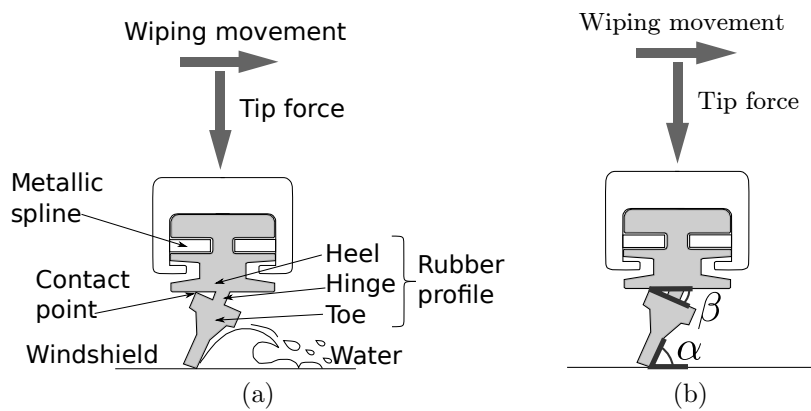


FIG. 2: Blade profile. (a) Description of the profile. (b) Functional requirements associated with the profile.

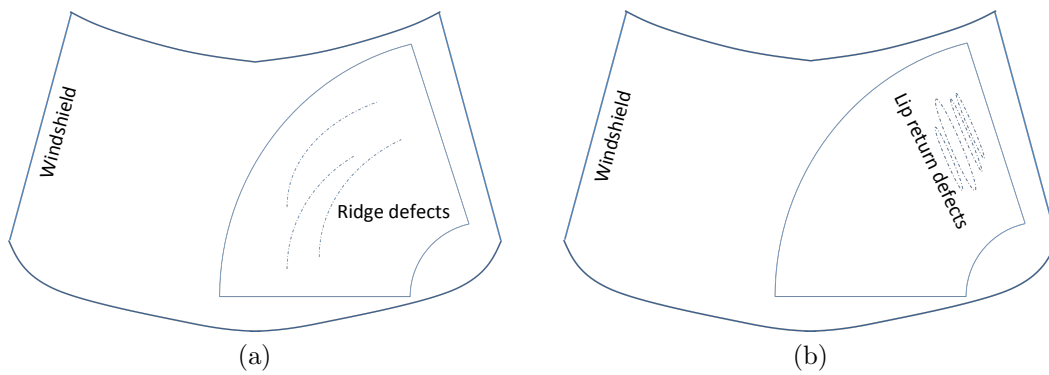
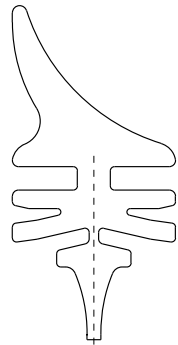
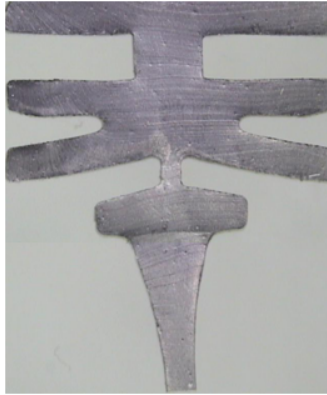


FIG. 3: Wiping defects



(a)



(b)

FIG. 4: (a) Reference cross-section of the blade as it appears in the drawings of the component. (b) Cross-section of a blade as obtained after extrusion (image courtesy of Valeo, copyright Valeo).

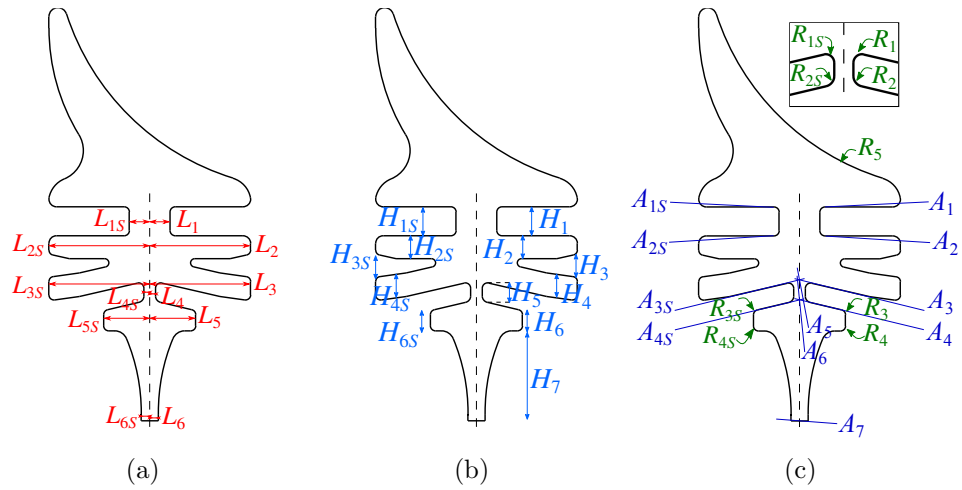


FIG. 5: Parameterization of the reference cross-section to take into account manufacturing uncertainties. (a) Length of subcomponents. (b) Height of subcomponents. (c) Angles and fillet radii.

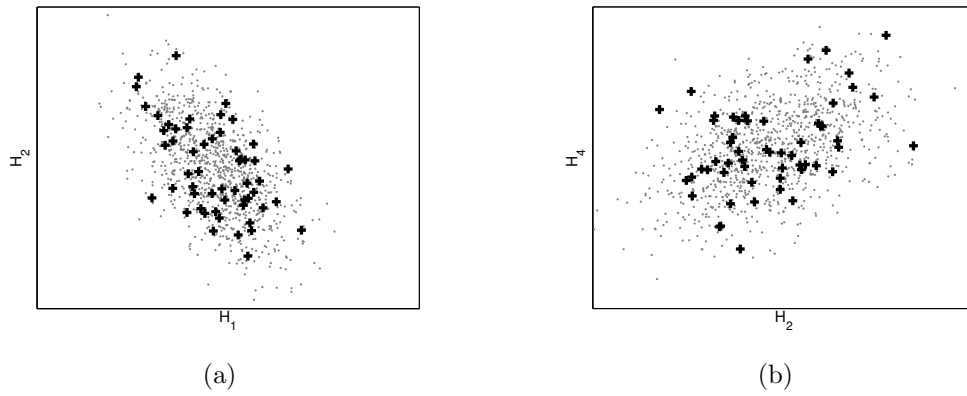


FIG. 6: Correlation between the dimensions. The black crosses represent the data measured on parts and the grey points represent 1000 samples generated using Monte Carlo simulation. (a) H_1 and H_2 . (b) H_2 and H_4 .

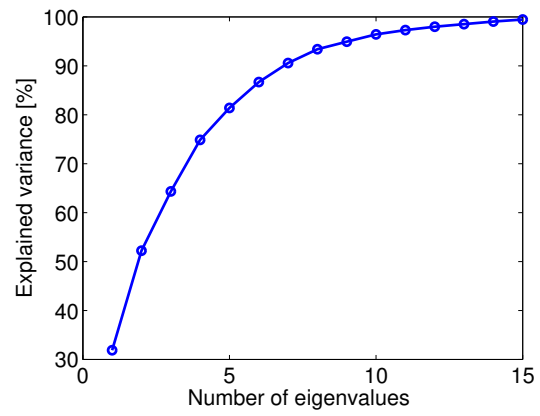
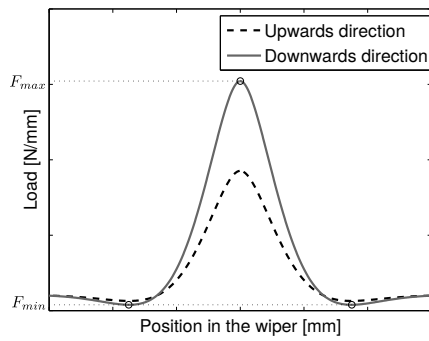
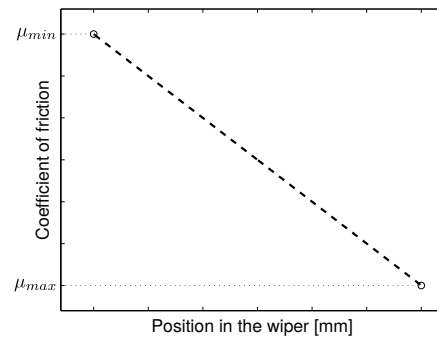


FIG. 7: Explained variance in terms of the number of eigenvalues used in the Karhunen-Loève expansion.



(a)



(b)

FIG. 8: (a) Variation in force with respect to position along the wiper blade. (b) Variation in the coefficient of friction between the blade and the windshield, expressed with respect to the position along the wiper blade.

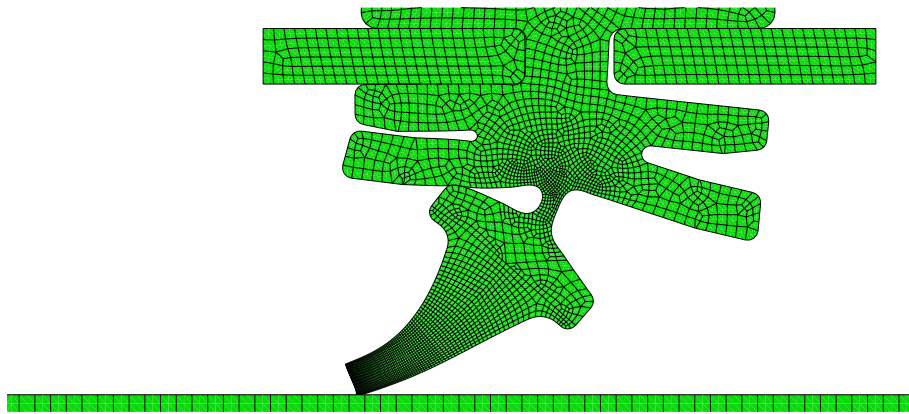


FIG. 9: Finite element model of the blade profile.

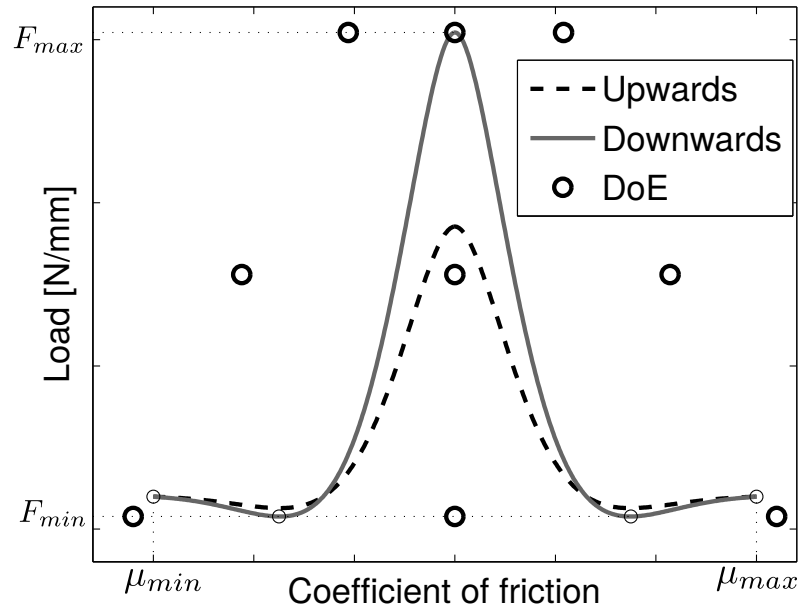


FIG. 10: Generation of the calibration set used for the response surfaces (hollow points).

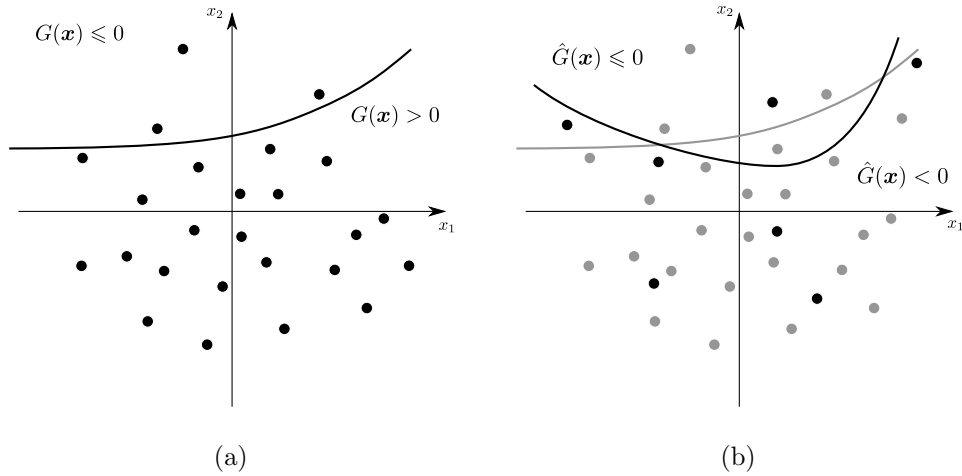


FIG. 11: Schematic representation of the reliability procedures. (i) Classification of samples (represented by the black points) into failure domain and safe domain. The thick black line represents the limit state. (b) Basic concept of the AK methods. The black points represent the enriched points where the performance function is evaluated; the gray points represent the samples where the surrogate model is used instead. The gray line represents the actual limit state, the black line represents the approximate limit state obtained using the surrogate model and used for the classification.

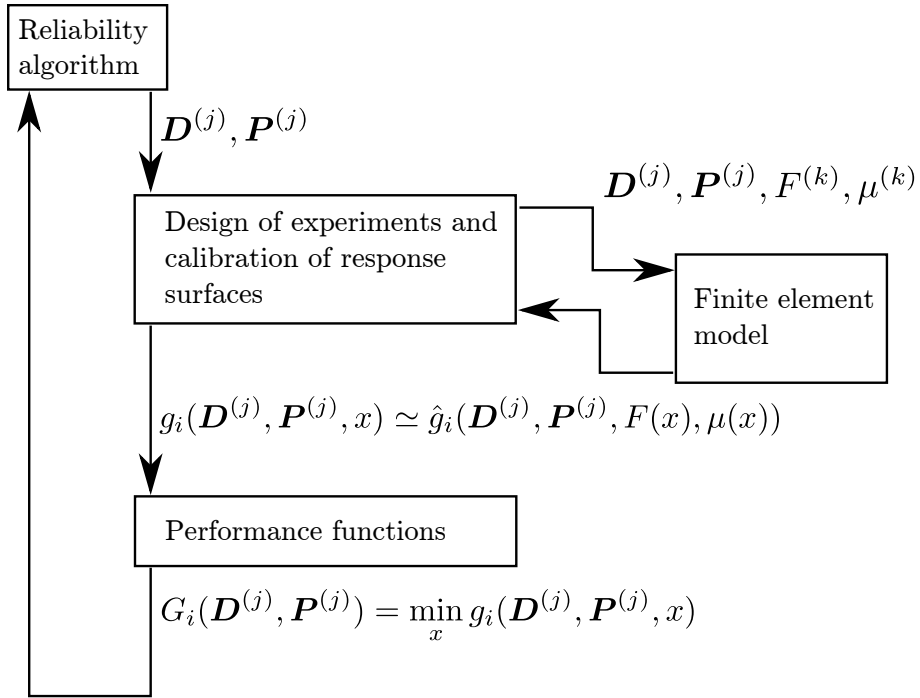


FIG. 12: Workflow of the procedure.

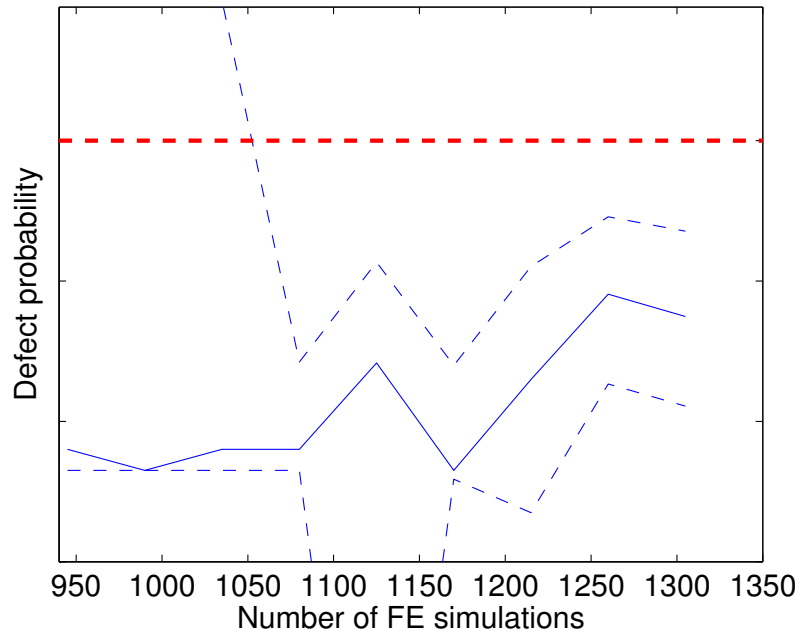


FIG. 13: Variation in defect probability (solid line) during the iterations of the AK method. The dashed line represents the confidence bounds of the defect probability; the thick dashed line represents the upper bound of the defect probability defined by the quality standards.